

OPEN

Nitrogen enrichment increases greenhouse gas emissions from emerged intertidal sandflats

Dallas J. Hamilton^{1,2}, Richard H. Bulmer², Luitgard Schwendenmann³ & Carolyn J. Lundquist^{1,2*}

Unvegetated, intertidal sandflats play a critical role in estuarine carbon and nutrient dynamics. However, these ecosystems are under increasing threat from anthropogenic stressors, especially nitrogen enrichment. While research in this area typically focuses on sediment-water exchanges of carbon and nutrients during tidal inundation, there remain significant gaps in our understanding of GHG (Greenhouse Gas) fluxes during tidal emergence. Here we use *in situ* benthic chambers to quantify GHG fluxes during tidal emergence and investigate the impact of nitrogen enrichment on these fluxes. Our results demonstrate significant differences in magnitude and direction of GHG fluxes between emerged and submerged flats, demonstrating the importance of considering tidal state when estimating GHG emissions from intertidal flats. These responses were related to differences in microphytobenthic and macrofaunal activity, illustrating the important role of ecology in mediating fluxes from intertidal flats. Our results further demonstrate that nitrogen enrichment of 600 gN m⁻² was associated with, on average, a 1.65x increase in CO₂ uptake under light (photosynthetically active) conditions and a 1.35x increase in CO₂ emission under dark conditions, a 3.8x increase in CH₄ emission and a 15x increase in N₂O emission overall. This is particularly significant given the large area intertidal flats cover globally, and their increasing exposure to anthropogenic stressors.

Unvegetated soft sediment habitats have been shown to play a critical role in carbon and nutrient dynamics within estuaries and the coast¹⁻⁴. These habitats are estimated to accumulate over 740,000 tonnes of carbon each year⁵, making significant contributions to reducing global carbon emissions. However, these ecosystems are under increasing threat due to stressors such as elevated nutrient loading sourced from anthropogenic activities such as agriculture and urbanization⁶⁻⁸.

Empirical measurements of fluxes on intertidal flats and the influence of nutrient enrichment on those fluxes have typically focused on the sediment-water column exchange of carbon and nutrients during tidal inundation (e.g. ^{2,3,9,10}). These submerged fluxes are subsequently used to infer fluxes during tidal emergence, either explicitly (e.g. ³) or implicitly (e.g. ¹). However, key drivers that influence GHG (greenhouse gas) fluxes (specifically CO₂, CH₄, and N₂O) on intertidal flats change significantly between tidal inundation and emergence, such as the benthic light climate¹¹, temperature¹², oxygen dynamics^{12,13}, and macrofaunal activity^{14,15}. If these drivers result in differences in GHG fluxes between submerged and emerged periods, upscaling from submerged fluxes to the full tidal cycle may result in inaccurate accounting of GHG budgets due to under- or over-estimates. Further uncertainties in GHG budgets for unvegetated intertidal flats occur due to the lack of understanding of the influence of nutrient enrichment on these habitats during tidal emergence, which could drive further differences in fluxes between submerged and emerged conditions.

The impact of nitrogen enrichment on estuaries is expected to worsen in the coming years (e.g. ^{7,16,17}). Consequently, reducing the uncertainty of estimates of the impact of nutrient enrichment on the flux of GHGs is an integral part of accurately quantifying GHG emissions from emerged intertidal flats. Here we investigate the impact of nutrient enrichment on GHG fluxes from emerged intertidal flats by manipulating sediment nutrient concentrations for several months at five sites on the North Island, New Zealand which vary in environmental characteristics. Three sites were selected in the Whangarei Harbour, with two sites in the Whangateau Harbour and the Raglan Harbour. Having three sites along an environmental gradient in the Whangarei Harbour allowed

¹Institute of Marine Science, University of Auckland, Auckland, New Zealand. ²National Institute of Water and Atmospheric Research Ltd (NIWA), Hamilton, New Zealand. ³School of Environment, University of Auckland, Auckland, New Zealand. *email: Carolyn.Lundquist@niwa.co.nz

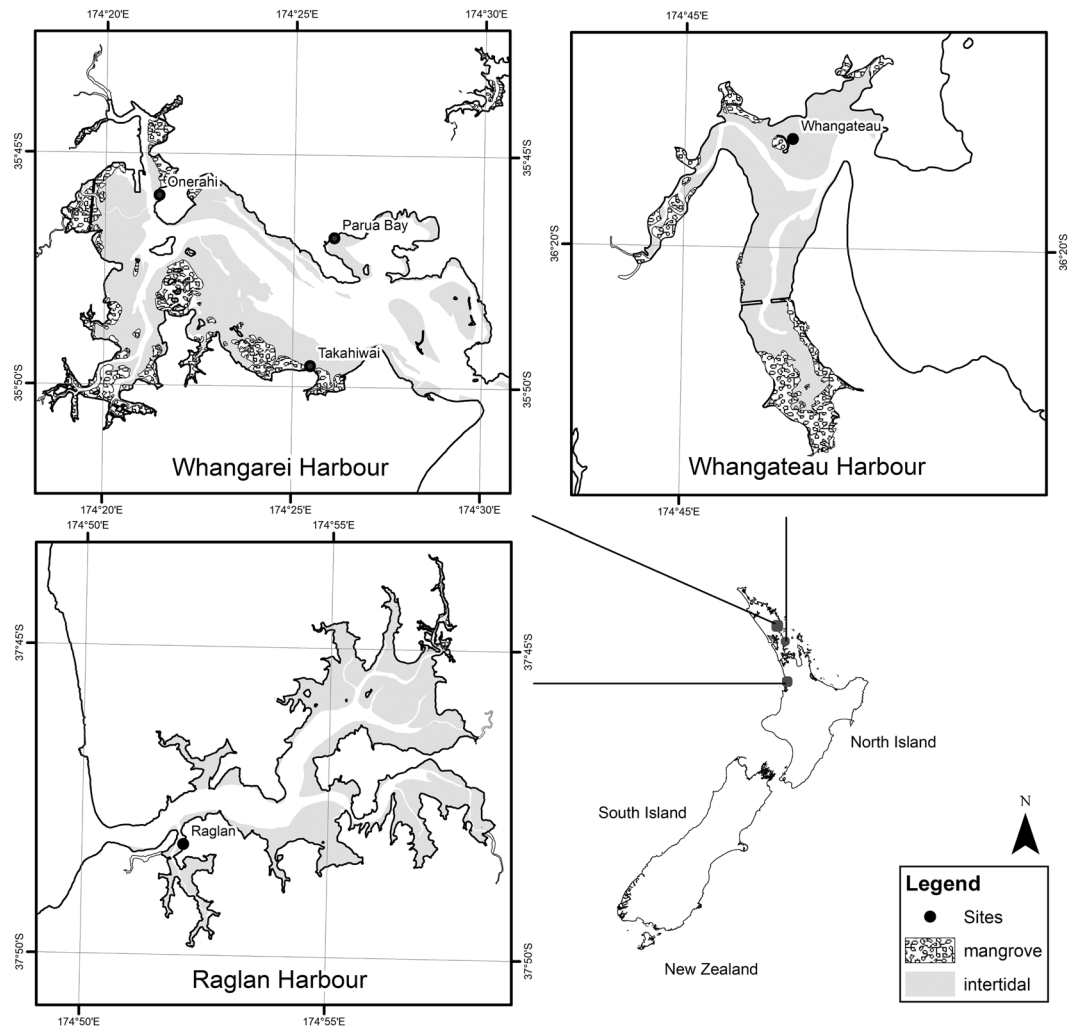


Figure 1. Study sites on the Whangarei, Whangateau, and Raglan Harbours in northern New Zealand.

generalisations to be made for one estuary, while having a further two sites in different estuaries provided information on whether those generalisations could be applied to different estuaries. Further, we compare these values to data collected by other researchers during tidal submergence, to improve our understanding of how tidal state may impact GHG fluxes on intertidal flats.

We hypothesised nutrient enrichment will increase the emission of CO_2 , CH_4 and N_2O . We also hypothesised that the flux of greenhouse gases from unvegetated intertidal flats will differ between periods of tidal emergence and periods of tidal submergence.

Methods

Study sites. Five sites across three estuaries were selected to span a range of environmental conditions (e.g. sediment mud content, organic matter content, chlorophyll concentrations, and macrofaunal community composition). Three of these sites were in the Whangarei Harbour, one was in the Raglan Harbour, and one was in the Whangateau Harbour (Fig. 1).

Whangarei Harbour is a large, unstratified estuary over 20 km long, covering an area of 104 km^2 ^{18,19} and with a catchment area of 229 km^2 ²⁰. Mean depth in the harbour is 4.42 m ²¹, with a mean tidal range of 1.73 m ¹⁸. Approximately 28% of the harbour flushes each tide, and about half (54 km^2) of the harbour area is intertidal^{20,21}. Approximately two thirds of the intertidal area is composed of unvegetated, intertidal flats, with the remainder being mangrove forest and seagrass meadows, both of which have expanded in recent decades^{22,23}. Land use in the catchment varies, with high proportions of pastoral agriculture and plantation forestry alongside urban areas and areas of native vegetation²⁰.

Whangateau Harbour is a shallow estuary of approximately 9.2 km^2 , with little freshwater input²⁴. The harbour has a high flushing rate, with up to 99% of the water being exchanged with each tide²⁴, and 85% of the harbour is composed of intertidal flats²⁵. The spring tidal range of the harbour is 2.2 m ²⁶. The harbour has a small catchment ($\sim 40 \text{ km}^2$ in area), comprised primarily of native forest, but with areas of plantation forestry, livestock agriculture, horticulture, and urban use²⁶.

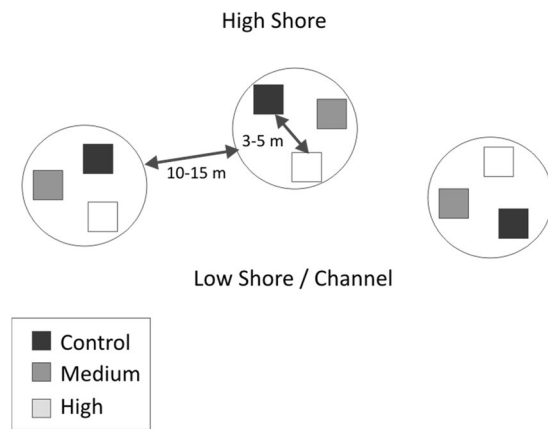


Figure 2. Example site layout of three replicate nutrient enrichment treatments. High Shore and Low Shore/Channel indicate proximity to terrestrial habitats, and toward open water, respectively.

Raglan Harbour is a drowned river valley of approximately 33 km² area, of which ~70% is intertidal. The harbour has a maximum depth of 18 m, although channel depths closer to 5 m are more common. Raglan Harbour has a neap tidal range of 1.8 m and a spring tidal range of 2.8 m with 50–75% of the volume of the Harbour being exchanged each tidal cycle (at neap and spring tides respectively). The catchment is large (165 km²), and is dominated by agriculture and plantation forestry which have historically resulted in large inputs of sediment, with small areas of native forest and urban areas²⁷.

Nitrogen enrichment treatments. At each site, three nutrient enrichment treatments were performed: a high N treatment (600 g N m⁻²), a low N treatment (150 g N m⁻²), and a control with no enrichment. The application method and treatment doses were based on a previously tested method of nitrogen enrichment in New Zealand intertidal flats, which successfully resulted in long term nitrogen enrichment at treated sites for periods of >6 months^{28,29}. Nitrogen fertiliser was placed in twenty 5 × 15 cm deep cores per m², using a controlled-release, nitrogen-only, urea fertiliser (with no potassium, phosphorous, or trace elements). Fertiliser was inserted at a depth of 15 cm, with sediment cores removed, fertiliser added, and sediment returned to fill the remainder of the hole created by the core. This enrichment procedure was carried out 6 months prior to GHG flux measurements, in order to avoid impacts of the physical disturbance effects of enrichment and to measure the effect of chronic nutrient enrichment on those fluxes, which have been observed to occur at 3–6 months post nutrient enrichment using the same methodology²⁹.

Each treatment plot was 3 × 3 m in area, and plots were separated by at least 3 m from any other plot within each replicate block (Fig. 2). Treatments were replicated three times at each site in a randomized block design, for a total of nine plots per site. Replicate blocks were situated 10–15 m apart. All plots were located at similar tidal heights (approximately four hours of tidal emergence), with distances in tidal height between treatment plots negligible relative to the tidal range. Measurements carried out using static chambers in Light/Dark pairs separated by 0.2 m within each plot (for a total of 18 benthic chambers per site) and were at least 1 m from plot edges to minimise edge effects across the edge of treatment plots. Chambers were arranged in Light/Dark pairs to capture respiration rates (dark chambers) and the impact of photosynthesis/production (light chambers) on GHG emissions.

Nutrient enrichment at all sites was performed in April 2017, followed by sampling of GHG fluxes in November and early December 2017. Two of the five sites (Raglan and Whangateau) were re-treated with nitrogen fertiliser in December 2017, and a second round of sampling was carried out at these sites (and in the control treatments of the three sites in Whangarei) in June and July 2018 to investigate seasonal variation in GHG fluxes.

Greenhouse gas flux measurement. GHG fluxes across the sediment-atmospheric interface were measured using 30 L, 0.25 m² airtight benthic chambers. The measurement chambers were arranged in Light and Dark pairs, with one chamber having a clear lid and one an opaque lid. As soon as the receding tide exposed the study site, chambers were pushed 7 cm into the sediment. After approximately 10 minutes, the lids (and dark covers for dark chambers) were attached and sealed, and 10 minutes after that the first gas sample was taken. The 20 minute period between chamber placement and the start of flux measurements was chosen as a result of a preliminary experiment for this study³⁰. As part of that experiment, the fluxes of GHGs were measured several times throughout the period of emergence at two sites with different environmental conditions, in order to determine the necessary sampling period for this study. The same light/dark paired *in situ* benthic chamber methods were used as those in this study, but with six gas samples collected from each chamber at approximately 25 minute intervals, instead of only collecting initial and final gas samples. This preliminary experiment showed no evidence of a large initial flux, with the flux of CO₂ and CH₄ over the first sampling period similar to that in the second and third period for each site, except for the CO₂ flux in the light chambers at Onerahi. This provided strong evidence that there was not a high initial flux of GHGs in the chambers resulting from the physical disturbance of placing the chambers in the sediment, as any impact from this disturbance would have been expected across all treatments at

all sites. Consequently, a 20-minute delay between the disturbance of placing the chamber and taking the initial measurement was used as a precaution but was considered adequate.

Initial 900 mL gas samples were collected from the chambers within ten minutes of sealing the chambers and stored in Tedlar bags. A final 900 mL gas sample was collected from each chamber immediately prior to tidal submergence at the site. The two samples in combination accounted for approximately 6% of the total 30 L volume of the measurement chamber. The period between the initial and final sampling of gases in the chambers ranged from 2–4 hours in length, depending on the magnitude of the tide, and the presence or absence of wind-driven waves that influenced the duration of tidal emergence/submergence.

Samples were kept in dark, insulated bins at ambient temperature and transported to the University of Auckland laboratory facilities for analysis. Gas samples were analysed within 24 hours of collection, using a Picarro G2508 Gas Analyser to determine the concentration of N₂O, CO₂, and CH₄ gas in the samples. The detection and accuracy limits of the Picarro analyser are listed in the Supplementary Information.

The samples were collected twice for at each site, once in November/December 2017 for all nutrient enrichment treatments, and once in June/July 2018 for all enrichment treatments at the Whangateau and Raglan sites and for the Control treatment at the three sites in Whangarei. More regular sampling was not feasible, in part due to the unavoidable physical disturbance of sampling. It is likely that this disturbance, if it occurred more regularly, would influence the processes at those sites³¹, altering the fluxes and potentially obscuring the effect of prolonged nutrient enrichment on GHG fluxes.

Flux calculations. Gas concentration measurements from the Picarro Gas Analyser were given in molar parts per million (ppm). To convert this to a standard gas flux ($\mu\text{mol m}^{-2} \text{hr}^{-1}$), the Ideal Gas Law was used, calculating the molar concentration of a gas at the start and end of the gas sampling and the consequent change over time (Eq. 1).

$$\text{flux} = \frac{\left(G_F \times \frac{P_F \times V}{R \times T_F}\right) - \left(G_I \times \frac{P_I \times V}{R \times T_I}\right)}{A \times \Delta t} \quad (1)$$

where G = concentration of a given GHG in the chamber at the start (I) and end (F) of the measurement (ppm); P = atmospheric pressure at the start (I) and end (F) of the measurement (atmosphere); V = volume of gas in the chamber (L); R = Ideal Gas Constant of 0.0821 L atm mol⁻¹ K⁻¹; T = temperature in the chamber at the start (I) and end (F) of the measurement (K); A = area of sediment covered by chamber (m²); and Δt = time between the start and end of the measurement (hours).

Site characteristics. While there are a multitude of environmental variables that may drive variation in the flux of GHGs, the following variables were selected with the aim of explaining the greatest possible proportion of variation in GHG fluxes with the limited resources available.

Temperature inside the chambers was recorded by 1-Wire i-button DS1921G-F5# automated loggers, located 10 cm from the edge of the chamber and 2 cm above the sediment surface. Photosynthetically Active Radiation (PAR) intensity was measured using two Odyssey Submersible PAR Loggers at each site.

Composite samples of five 2 cm deep, 2.5 cm diameter cores were collected from within 30 cm of the outer edge of each paired light and dark chambers to characterize sediment properties. To calculate pore water content, an approximately 15 g subsample was homogenised, weighed, freeze-dried for 8 days, and weighed again. The difference in weight between samples was calculated, and the proportion of the sample comprised from water expressed as a percentage. Chlorophyll a was analyzed by freeze drying an ~15 g subsample of homogenised sediment, producing approximately 5 g of dry sediment. Samples were boiled in 90% ethanol to extract chlorophyll a³². The extract was processed with a spectrophotometer (Shimadzu UV Spectrophotometer UV-1800). Samples were then acidified to separate phaeophytin from chlorophyll a³³. The chlorophyll-a and phaeophytin content of the sediment is an indication of the microphytobenthic biomass that can occur at each site^{34,35}. Due to resource constraints, more comprehensive measures of microbial activity could not be carried out. As such, the chlorophyll-a and phaeophytin content of the sediment are to be used implicitly as proxies for microbial activity.

Organic matter content was estimated using an ~5 g subsample of freeze-dried, homogenized sediment which was weighed, ashed at 450 °C for four hours³⁶, and reweighed. Organic matter was calculated from the difference between dry and ashed weights. While attempts were made to measure the dissolved inorganic nitrogen concentration in the pore water at each site, due to analytical problems that data was unusable. As a result, the organic matter content of the sediment was used as a proxy.

Sediment grain size was measured using a Malvern Mastersizer 3000 (measuring particles 0.1–3500 μm in diameter). Samples were digested in 10% hydrogen peroxide until frothing ceased, rinsed with distilled water in a centrifuge, and run through the Malvern. The mud content was measured as the proportion of grains <63 μm in diameter.

Macrofaunal community characteristics have been found to be important factors influencing the flux of GHGs on temperate intertidal flats, with the abundance of large bioturbating bivalves being key drivers of this influence^{15,37}. Consequently, the macrofaunal community characteristics were sampled once in summer and once in winter for each pair of Light/Dark chambers, using one 15 cm deep, 13 cm diameter sediment core immediately adjacent to the paired chambers (within the treatment plot). Cores were sieved on a 500 μm mesh. For the samples collected during summer, the material retained was preserved in 50% isopropyl alcohol and stained with Rose Bengal for subsequent analysis. All macrofaunal organisms observed were counted and identified to the lowest taxonomic level possible – in most cases species. Macrofaunal sampling in winter was limited to counts and measurements of bivalves >5 mm diameter (*Austrovenus stutchburyi*, *Macomona liliana*, and *Paphies australis*); material was returned to the sampling site.

	Onerahi		Parua Bay				Takahiwai				Whangateau				Raglan					
	Summer	Winter	Summer	Winter	Summer	Winter	Summer	Winter	Summer	Winter	Summer	Winter	Summer	Winter	Summer	Winter				
Physical																				
Temperature (°C)	22	(0.80)	20.8	(2.40)	21.1	(1.70)	19.6	(1.30)	17.5	(0.70)	20.7	(5.50)	23.2	(1.00)	20.8	(2.20)	22	(0.80)	13.2	(0.90)
Light intensity (umol photon m ⁻² s ⁻¹)	984		2323		1670		2604		426		3085		NA		1927		420		1192	
Sediment																				
Mud content (%)	5.9	(1.00)	9.1	(0.09)	7.8	(3.10)	12.3	(3.39)	1.5	(1.20)	1.7	(1.13)	3.5	(0.90)	9.7	(1.94)	17.5	(2.30)	20.4	(2.26)
Organic Matter (%)	1.8	(0.20)	1.2	(0.20)	2.2	(0.20)	1.7	(0.10)	1.4	(0.10)	1	(0.10)	1.4	(0.10)	1.1	(0.10)	3.9	(0.20)	2.7	(0.30)
Porosity (%)	0.49	(0.02)	0.49	(0.02)	0.45	(0.03)	0.45	(0.03)	0.47	(0.02)	0.47	(0.02)	0.47	(0.01)	0.47	(0.01)	0.53	(0.03)	0.53	(0.03)
Microphytobenthos																				
Chl a (dw mg g ⁻¹ sediment)	8.8	(1.40)	5.8	(0.70)	6.1	(1.20)	7.8	(2.20)	8.4	(2.00)	8	(0.30)	10.7	(2.70)	12.9	(3.10)	17.2	(5.90)	15.4	(2.10)
Phaeophytin (dw mg g ⁻¹ sediment)	3.2	(0.50)	3.1	(0.20)	2.6	(0.50)	3.5	(0.80)	3	(0.80)	3.6	(0.50)	3.2	(0.80)	5	(1.80)	9	(4.90)	7.1	(0.70)
Macrofauna																				
<i>Macomona liliana</i>	1.1	(1.00)	0.3	(0.50)	2.1	(2.10)	3	(0.00)	4.1	(2.90)	3	(0.90)	3.1	(2.60)	0.7	(0.70)	1.8	(1.80)	0.3	(0.50)
<i>Austrovenus stutchburyi</i>	3.9	(2.60)	0	(0.00)	14.8	(7.20)	5.3	(2.10)	12.2	(5.80)	7.3	(2.70)	37.4	(18.40)	10.7	(2.40)	55.6	(15.10)	18.6	(11.20)
Total bivalves	5	(2.80)	0.3	(0.50)	16.9	(7.90)	8.3	(2.10)	16.3	(7.80)	10.3	(3.60)	40.7	(20.50)	11.4	(2.70)	57.4	(15.60)	18.9	(11.30)

Table 1. Site characteristics (mean \pm standard deviation) for each site and in each season where gas flux measurements were carried out.

Statistical analysis. The PERMANOVA + package for PRIMER v7 was used to quantify differences in the environmental variables measured at different sites and in different seasons, and to quantify differences in the flux of GHGs between and within sites, nutrient treatments, light exposure (i.e. Light or Dark chambers), and seasons.

Permanovas were carried out on Euclidian Distance Resemblance matrices, using the fixed factors of Site (Onerahi, Parua Bay, Takahiwai, Raglan, and Whangateau), Treatment (Control, Medium, or High nutrient enrichment), Light Exposure (Light or Dark), and Season (Summer or Winter) for the GHG fluxes.

For environmental variables, the factors of Site and Season were used. The highest order interaction that was significant at the $p < 0.05$ level was used to analyse differences in flux between groups of these factors. After an interaction was identified, post-hoc pairwise tests were carried out to identify which groups within those interactions were significantly different at the $p < 0.05$ level, and the direction of those differences.

Results

Site characteristics. The sites used in this study differed significantly in their environmental conditions ($p < 0.05$), exhibiting a gradient of environmental conditions (Table 1). Temperature, sediment mud content ($< 63 \mu\text{m}$), sediment organic matter content, sediment porosity, and chlorophyll and phaeophytin concentration generally were lowest at Takahiwai, and highest at Raglan, with Onerahi, Parua Bay, and Whangateau exhibiting intermediate values (Table 1).

The sites differed in environmental conditions between summer and winter sampling, with sites generally having lower temperatures, organic matter content, and lower bivalve abundance in winter than in summer (Table 1), and higher mud content, chlorophyll, and phaeophytin concentration in winter (Table 1). However, the summer of 2016–2017 was an especially wet summer, with higher than average rainfall and lower than average daily temperatures. Also, the 2018 winter was an especially mild winter, with warm temperatures and clear skies for much of the season. This may have resulted in a smaller difference in environmental conditions between seasons than would usually be expected at these sites. Temperatures inside the chambers typically varied by 2–3 degrees in dark chambers and 3–4 degrees in light chambers over the duration of the chamber placement. The temperatures inside the chambers were on par with those outside the chambers, and did not reach temperatures higher than those that would be expected on the flats on a calm, fine day in the season the fluxes were measured.

Greenhouse gas fluxes. At the non-enriched (control) sites, under Light conditions, $172 \pm 76 \mu\text{mol m}^{-2} \text{h}^{-1}$ of CO_2 was removed from the atmosphere, while under dark conditions $183 \pm 56 \mu\text{mol m}^{-2} \text{h}^{-1}$ of CO_2 was emitted. This gave an average net primary productivity (NPP) of $355 \pm 132 \mu\text{mol m}^{-2} \text{h}^{-1}$. For this study, CO_2 flux data is presented as separate light and dark fluxes instead of as NPP, as expressing the fluxes as NPP would not show the actual amount of CO_2 being emitted (or taken up) by the intertidal flats, which is the key interest for this study. NPP can be inferred from the data already presented in this manuscript by simply subtracting the CO_2 flux under dark conditions from the CO_2 flux under light conditions.

No effect of Light or Dark treatment was observed for the CH_4 or N_2O fluxes, with emissions of $0.050 \pm 0.14 \mu\text{mol m}^{-2} \text{h}^{-1}$ and $0.004 \pm 0.0148 \mu\text{mol m}^{-2} \text{h}^{-1}$ respectively.

CO_2 . For all nutrient treatments, at all sites, in all seasons, the chambers under Light conditions had significantly lower CO_2 emissions (or higher uptake) than the chambers in Dark conditions (Fig. 3). The CO_2 fluxes in Light conditions ranged from -0.1 to $-670 \mu\text{mol m}^{-2} \text{h}^{-1}$ with a mean of $-233 \mu\text{mol m}^{-2} \text{h}^{-1}$. In Dark conditions, the fluxes ranged from 2 to $890 \mu\text{mol m}^{-2} \text{h}^{-1}$ with a mean of $213 \mu\text{mol m}^{-2} \text{h}^{-1}$.

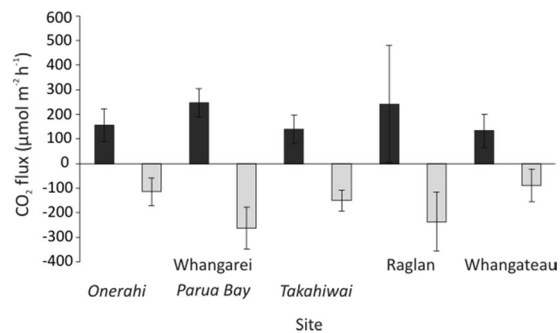


Figure 3. CO₂ flux in the Control treatments for each site across both seasons sampled (mean ± standard deviation). Black bars represent Dark chambers, while light grey bars represent Light chambers.

In Light chambers, the CO₂ uptake in Control treatments was significantly lower (i.e. less CO₂ emission) than in the Medium and High N enrichment treatments, which were not significantly different to each other (Table 2, Fig. 4). There were no significant differences due to nutrient enrichment on the flux of CO₂ in Dark chambers (Table 2).

In Light chambers in summer, the CO₂ flux at Raglan was significantly smaller (i.e. more negative) than any other site except Takahiwai, and the CO₂ flux at Whangateau was significantly ($p < 0.05$) higher than any other sites (Table 2). In the Dark chambers during summer, Takahiwai had significantly smaller emissions of CO₂ than any other sites, and there were no significant differences between any other sites. In winter, no significant differences were observed between sites (Table 2).

There was a seasonal effect on the flux of CO₂ at Raglan and Whangateau, with the Dark chambers at Raglan and both the Light and Dark chambers in Whangateau having significantly smaller CO₂ fluxes in winter than in summer ($p < 0.05$) (Table 2). In contrast, Light chambers in Raglan showed significantly smaller (i.e. larger negative) CO₂ fluxes in summer than in winter (Table 2).

CH₄. The CH₄ fluxes ranged from 0.82 to $-0.65 \mu\text{mol m}^{-2} \text{h}^{-1}$, with a mean of $0.11 \mu\text{mol m}^{-2} \text{h}^{-1}$. There was a significant Site and Nutrient Treatment interaction, with significantly lower CH₄ fluxes in the Control treatment than the High treatment at all sites except Parua Bay ($p < 0.05$). Overall, there were no significant differences in CH₄ flux between Light and Dark conditions (Fig. 5, Table 3).

For the Control N enrichment treatment, the fluxes at Raglan were significantly smaller than the fluxes at either Parua Bay or Whangateau, and the fluxes at Takahiwai were also significantly smaller than the fluxes at Whangateau (Fig. 6, Table 3). There were no significant differences between sites for the Medium treatments, but for the High treatments Onerahi and Parua Bay both had significantly smaller CH₄ fluxes than Raglan (Table 3). There were no significant differences between Control and Medium enrichment treatments at any sites except Raglan, and at Parua Bay there were no significant differences in CH₄ flux between any enrichment treatments (Table 3).

N₂O. The N₂O fluxes ranged from 0.84 to $-0.44 \mu\text{mol m}^{-2} \text{h}^{-1}$, with a mean of $0.03 \mu\text{mol m}^{-2} \text{h}^{-1}$ (Fig. 7). There were two significant three-way interactions: a Site by Nutrient Treatment by Light Treatment interaction, and a Site by Nutrient Treatment by Season interaction (Table 4). There was a significant 4-way interaction between Site, Nutrient Treatment, Light Treatment, and Season ($p < 0.05$), though post-hoc pairwise tests showed no significant differences between any two groups in that interaction (Table 4).

The N₂O flux at both Parua Bay and Raglan increased with nutrient enrichment in both seasons, with the lowest fluxes in Control treatments, and the largest N₂O fluxes in High nutrient treatments (Fig. 7b,d). Across all three nutrient treatments, and in both Light and Dark conditions, Whangateau had consistently smaller fluxes of N₂O than other sites (Fig. 7e). Additionally, the chambers at both Raglan and Whangateau with High nutrient enrichment had significantly larger fluxes of N₂O in the Light chambers than in the Dark (Table 4).

For the Site by Nutrient Treatment by Season interaction, nutrient enrichment was found to increase the flux of N₂O in Parua Bay in summer (Fig. 7b), and in Raglan in both Summer and Winter (Fig. 7d). The only N₂O fluxes that were significantly different between seasons were those in Raglan, with the N₂O fluxes observed in Winter being significantly larger than those observed in Summer for all three nutrient treatments (Fig. 7d). In the Medium and High N enrichment treatments in both Summer and Winter, Whangateau consistently had significantly smaller fluxes of N₂O (Fig. 7e), and Raglan had significantly larger fluxes of N₂O (Fig. 7d, Table 4).

Discussion

This study is the first to demonstrate that nitrogen enrichment is associated with an increase in CO₂ uptake and CH₄ and N₂O emissions from emerged unvegetated flats, providing valuable new insights on the impact of nutrient enrichment on estuaries. This study also indicated that tidal emergence is associated with differences in the magnitude and direction of GHG fluxes when compared to fluxes measured during tidal submergence, improving our understanding of the role emerged intertidal flats play in estuarine GHG fluxes.

Nutrient enrichment of 600 gN m^{-2} was associated with an average of 1.65x increase in CO₂ uptake under light conditions and 1.35x increase in the average CO₂ emission in dark conditions (although the latter was not

Term	df	Pseudo-F	p(Perm)	Post hoc tests		
Site × nutrient	8	0.96203	0.4772			
Site × light	4	8.3302	0.0001			
Site × Season	4	1.0338	0.3937			
nutrient × light	2	6.6977	0.0014	Light	Control	
				C < M = H	L < D	
				Dark	Medium	
					L < D	
					High	
					L < D	
nutrient × Season	2	0.67088	0.5144			
light × Season	1	9.4367	0.002			
Site × nutrient × light	8	1.9591	0.0569			
Site × nutrient × Season	2	0.052131	0.9486			
nutrient × light × Season	2	1.2485	0.2904			
Site × light × Season	4	4.9939	0.0015	Light, Summer	Onerahi, Summer	Raglan, Light
				(RAG = TAK) < ONE < WHT,	L < D	S < W
				RAG < PB < WHT	Parua Bay, Summer	Raglan, Dark
				Dark, summer	L < D	W < S
				TAK < (RAG = WHT)	Parua Bay, Winter	Whangateau, Light
					D = L	W < S
					Takahiwai, Summer	Whangateau, Dark
					L < D	W < S
					Raglan, Summer	
					L < D	
					Raglan, Winter	
					L < D	
					Whangateau, Summer	
					L < D	
					Whangateau, Winter	
					L < D	

Table 2. PERMANOVA results comparing fluxes of CO₂ as a function of different factors (site, nutrient enrichment treatment, light/dark conditions, and season). Significant effects (α = 0.05) are given in bold, and post-hoc pairwise tests are given for significant interactions. Significant interactions are prioritised over main effects, and three-way interactions over two-way interactions. C – Control nutrient treatment, M – Medium nutrient treatment, H – High nutrient treatment, RAG – Raglan site, TAK – Takahiwai site, ONE – Onerahi site, PB – Parua Bay site, WHT – Whangateau site, L – Light conditions, D – Dark conditions, S – Summer, W – Winter.

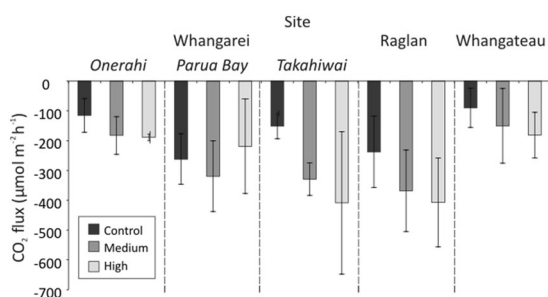


Figure 4. Mean CO₂ flux averaged across seasons for each nutrient enrichment treatment (Control, Medium, High) at each site under Light conditions, mean ± standard deviation.

statistically significant). High N enrichment was also associated with a 3.8x increase in CH₄ emission and a 15x increase in the emission of N₂O under both light and dark conditions.

There have been several studies linking microphytobenthic activity to GHG emissions, with some estimates finding them responsible for as much as 50% of all estuarine primary production (i.e. CO₂ flux) across all intertidal habitats³⁸. These results suggest that nutrient enrichment enhanced microphytobenthic activity and resulted in a modest net reduction in CO₂ emissions (driven by increased photosynthetic uptake) at our sites. However,

Term	df	Pseudo-F	p(Perm)	Post hoc tests		
Site x nutrient	8	2.4779	0.0173	Control	Onerahi	
				RAG<WHT=PB,	C<H	
				TAK<WHT	Takahiwai	
				High	C<H	
				(ONE=PB)<RAG	Raglan	
					C<M<H	
					Whangateau	
					C<H	
Site x light	4	0.29948	0.8814			
Site x Season	4	1.0919	0.3636			
nutrient x light	2	1.8386	0.1717			
nutrient x Season	2	0.41859	0.6679			
light x Season	1	0.13413	0.7135			
Site x nutrient x light	8	1.5039	0.1709			
Site x nutrient x Season	2	1.4792	0.236			
nutrient x light x Season	2	1.1182	0.3264			
Site x light x Season	4	3.843	0.0081	Light, Summer	Onerahi, Summer	Raglan, Light
				ONE<TAK<RAG,	L<D	W<S
				ONE<PB=WHT	Raglan, Summer	Raglan, Dark
				Dark, summer	D<L	S<W
				RAG<(ONE=WHT)	Raglan, Winter	Whangateau, Dark
				Dark, Winter	L<D	W<S
				WHT<RAG		

Table 3. PERMANOVA results comparing fluxes of CH₄ as a function of different factors (site, nutrient enrichment treatment, light/dark conditions, and season). Significant effects ($\alpha = 0.05$) are given in bold, and post-hoc pairwise tests are given for significant interactions. Significant interactions are prioritised over main effects, and three-way interactions over two-way interactions. C – Control nutrient treatment, M – Medium nutrient treatment, H – High nutrient treatment, RAG – Raglan site, TAK – Takahiwai site, ONE – Onerahi site, PB – Parua Bay site, WHT – Whangateau site, L – Light conditions, D – Dark conditions, S – Summer, W – Winter.

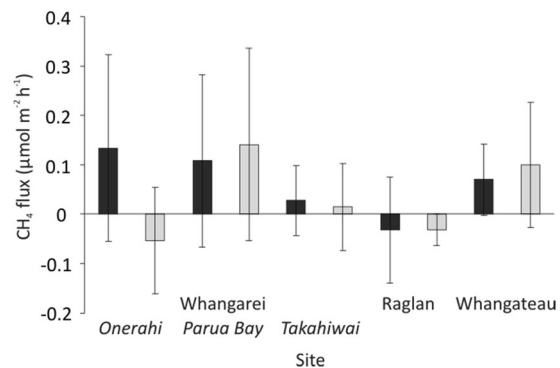


Figure 5. CH₄ flux in the Control treatments for each site, averaged across seasons, mean \pm standard deviation. Black bars represent Dark conditions, while light grey bars represent Light conditions.

this reduction in CO₂ did not offset the significant increase in the emission of CH₄ and N₂O – both of which are likely also a result of increased microbial activity, as both methanogenesis and denitrification (the processes responsible for a majority of CH₄ and N₂O emissions respectively^{1,4,39}) are controlled by microbial activity in the sediment³⁷.

After accounting for the relative impact of each gas on the greenhouse effect by converting CH₄ and N₂O into CO₂ equivalents (CH₄ is 25x more potent than CO₂ as a GHG; N₂O is 298x more potent than CO₂ as a GHG⁴⁰), an estimated average of the equivalent of 8.5 $\mu\text{mol m}^{-2} \text{h}^{-1}$ of CO₂ was emitted to the atmosphere from control sites under emerged conditions (allowing for both light and dark conditions). Nutrient enrichment resulted in an increase of 55% to 13.2 $\mu\text{mol m}^{-2} \text{h}^{-1}$ of CO₂ equivalents.

This study was carried out alongside another experiment measuring the flux of O₂ (and by proxy CO₂, as one flux can be converted to the other with an approximate 1: -1 ratio⁴¹) under submerged conditions at the same sites⁴². Under Light conditions, the submerged sand flats emitted an average of over 100 $\mu\text{mol CO}_2 \text{m}^{-2} \text{h}^{-1}$ ⁴². In contrast, emerged sediment from this study has taken up approximately 180 $\mu\text{mol CO}_2 \text{m}^{-2} \text{h}^{-1}$. These results suggest that, at least at these study sites, sediments may switch between being a source of CO₂ during tidal

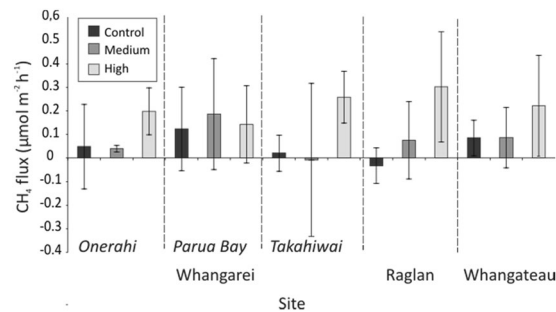


Figure 6. CH_4 flux at each nutrient treatment at each site, mean \pm standard deviation, with the measurements in Light and Dark conditions combined.

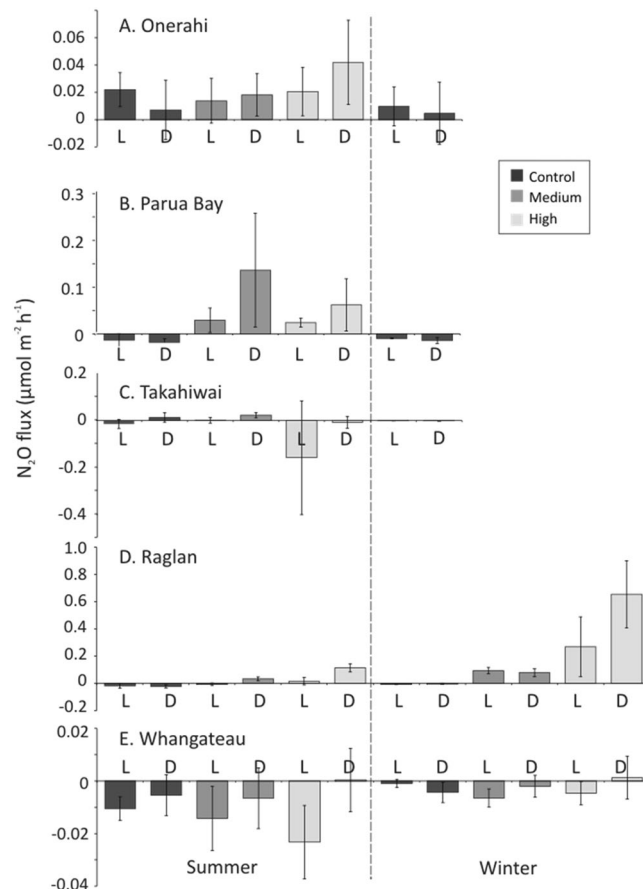


Figure 7. N_2O flux ($\mu\text{mol m}^{-2} \text{h}^{-1}$) within light (L) and dark (D) chambers for each of N enrichment treatments (Control, Medium, High), within each season (mean \pm standard deviation). A. Whangarei Harbour, Onerahi; B. Whangarei Harbour, Parua Bay; C. Whangarei Harbour, Takahiwai; D. Raglan; E. Whangateau.

submergence, to a sink of CO_2 during tidal emergence. This may be due to the higher light intensity available at the surface of the sediment under emerged conditions^{11,43}, allowing higher rates of photosynthesis by the microphytobenthos and lower rates of ventilation (meaning lower rates of CO_2 release) by macrofauna such as bivalves under emerged conditions⁴⁴.

While comparable submerged CH_4 and N_2O data was not collected at the same site, emerged fluxes in this study differ from submerged fluxes in other studies. Emerged CH_4 fluxes in this study were on average 2.8x lower, and N_2O fluxes on average 120x lower than submerged values reported elsewhere (Table 5). The differences in fluxes are consistent with the literature and likely driven by differences in environmental conditions. For example, in comparison to our study, CH_4 and N_2O emissions by Li *et al.*² were approximately 3x and 5x higher, however sediment organic matter content was 8–8.5%, approximately 3–8x higher than our study. Sediment organic matter content is positively associated with rates of nutrient cycling, which drive increased N_2O emissions^{4,15,45}, and with microbial production of CO_2 and CH_4 ^{46,47}. Macrofaunal community composition also varied significantly

Term	df	Pseudo-F	p(Perm)	Post hoc tests		
Site × nutrient	8	9.2892	0.0001			
Site × light	4	1.8507	0.1208			
Site × Season	4	6.5366	0.0003			
nutrient × light	2	4.0796	0.0183			
nutrient × Season	2	15.665	0.0001			
light × Season	1	0.67849	0.4221			
Site × nutrient × light	8	2.0812	0.0462	Control, Dark	Parua Bay, Light	Raglan, High
				(PB = TAK = RAG = WHT) < ONE	C < M < H	D < L
				Control, Light	Parua Bay, Dark	Whangateau, High
				PB < WHT < TAK, PB < ONE,	C < M < H	D < L
				(WHT = RAG) < TAK	Raglan, Light	
				Medium, Dark	C < M < H	
				WHT < (ONE = PB = RAG)	Raglan, Dark	
				Medium, Light	C < M < H	
				WHT < (ONE = PB = RAG)		
				High, Dark		
				WHT < (ONE = PB = TAK = RAG)		
				High, Light		
				WHT < (ONE = PB = TAK = RAG)		
Site × light × Season	4	0.58657	0.6637			
nutrient × light × Season	2	2.7951	0.0619			
Site × nutrient × Season	2	14.966	0.0001			
				Control, Summer	Parua Bay, Summer	Raglan, Control
				ONE < (OB = RAG = WHT)	C < (M = H)	S < W
				Control, Winter	Raglan, Summer	Raglan, Medium
				PB < RAG < TAK, PB < (RAG = ONE = WHT)	C < M < H	S < W
				Medium, Summer	Raglan, Winter	Raglan, High
				WHT < (ONE = PB = RAG), (WHT = TAK) < PB	C < M < H	S < W
				Medium, Winter		
				WHT < RAG		
				High, Summer		
				WHT < (TAK = ONE = PB), TAK < RAG		
				High, Winter		
				WHT < RAG		
Site × nutrient × light × Season	2	3.2761	0.0455	No significant pairwise differences at p < 0.05 level		

Table 4. PERMANOVA results comparing fluxes of N₂O as a function of different factors (site, nutrient enrichment treatment, light/dark conditions, and season). Significant effects ($\alpha = 0.05$) are given in bold, and post-hoc pairwise tests are given for significant interactions. Significant interactions are prioritised over main effects, and three-way interactions over two-way interactions. C – Control nutrient treatment, M – Medium nutrient treatment, H – High nutrient treatment, RAG – Raglan site, TAK – Takahiwai site, ONE – Onerahi site, PB – Parua Bay site, WHT – Whangateau site, L – Light conditions, D – Dark conditions, S – Summer, W – Winter.

between sites in this study, and with other studies, such as Kang *et al.*³⁹. Macrofauna influence the flux of CO₂, CH₄, and N₂O through several processes, such as increasing CO₂ emissions directly by increasing microbial respiration, and bioturbating the sediment^{15,48,49}. Variability in the activity of macrofauna may also drive differences in GHG flux rates between tidal emergence and submergence. For example, both CH₄ and N₂O are produced within the sediment, CH₄ via methanogenesis^{1,50} and N₂O as part of the denitrification process^{3,4,10}. The delivery of these gases to the sediment-atmosphere or sediment-water interface is accelerated by bioturbation (a process

Intertidal Habitat	Mean Reported Flux ($\mu\text{mol m}^{-2}\text{h}^{-1}$)			Flux measurement period	Reference
	CO ₂ *	CH ₄	N ₂ O		
Intertidal unvegetated flat (during emergence)	-172 ± 76	0.05 ± 0.14	0.006 ± 0.015	~2–3 hour	This study
	-1967 ± 1656			20–35 minute	55
	-2267 ± 1070			5 minute	11
			-0.29 ± 1.2	sediment core	4
			-0.25 ± 0.7	1.5 hour benthic	10
		5.3 ± 42		2 hour	39
Intertidal unvegetated flat (during submergence)			1.5 ± 3.7	1.5 hour	10
		0.14 ± 0.06	0.29 ± 0.19	5 hour	2
			0.36 ± 1.13	Meta analysis of 10 studies	3
	-974 ± 870			4 hour	11
	-1110 ± 636			6 hour	9
	110 ± 2386				42
Seagrass		48 ± 142		24 hour sediment cores	59
		11 ± 6		6 hour	60
	-5419 ± 3785			4 hour	11
			0.705 ± 1.12	Meta-analysis of 17 studies	3
Mangroves	206 ± 146			4 hour	61
	-1258 ± 3620	74 ± 705	2.4 ± 3.0	Meta-analysis of 18 studies	62
			0.44 ± 2.5	Meta-analysis of 17 studies	3
Saltmarsh		3.5 ± 4.1		Meta-analysis	63
	3122 ± 4302	2		Meta-analysis	64
			4.15 ± 7.65	1.5 hour	10
			2.8 ± 6.3	3 hour	65

Table 5. Mean GHG flux reported from different intertidal habitats including results from this study and the corresponding experiment during tidal submergence⁴², and other global studies. *Average CO₂ fluxes reported from measurements under light conditions.

largely driven by bivalves on intertidal flats in NZ⁵¹. Most bivalves, especially *A. stutchburyi* and *M. liliiana* (the two most commonly occurring bivalves in this study), are known to reduce their activity during tidal emergence (e.g.^{14,52}). This may decrease the delivery of GHGs from deeper in the sediment to the sediment surface. In addition, methodological differences may have contributed to differences between studies. For instance, Kang *et al.*³⁹ have taken sediment in the field and incubated them in the laboratory for two hours, whereas our study used *in situ* chambers placed over the sediment surface for up to >3 hours, with minimal disturbance to the sediment column. Disturbance to the sediment column may impact O₂ concentrations and expose anoxic sediment to oxygen^{15,48}, enhancing GHG production^{53–55}. The methods used in this study were established by a pilot study carried out in Hamilton³⁰. Part of that preliminary experiment was to measure the flux of GHG several times throughout the period of emergence, in order to determine the ideal sampling period. The same *in situ* incubation methods were used, but with six gas samples collected at approximately 25-minute intervals, instead of only collecting initial and final gas samples from each chamber. There has been research identifying the potential influence of the ebb and flood tide on the emission of GHGs on intertidal flats through ‘tidal pumps’^{39,56}. Based on this research, and on the results of the preliminary experiment described above³⁰, GHG flux sampling for this experiment was conducted over both the incoming and outgoing tides to capture any ‘tidal pump’ impact on the emission of these gases. This provides a robust measurement of the net GHG flux on unvegetated intertidal flats over the whole emerged period, allowing the upscaling of these fluxes to larger time scales, such as days, weeks, or years.

Our study showed that GHG fluxes from intertidal habitats are lower per m² than other coastal habitats, such as salt marsh, mangroves, or seagrass (Table 5). However, intertidal sandflats often cover vast areas within estuaries⁵⁷, and in these instances the contribution of intertidal flats to estuarine GHG fluxes is substantial. To demonstrate this, we calculate the contribution of intertidal flats to estuarine GHG emissions using a typical estuary from northern New Zealand as a case study (Tairua Harbour). After accounting for the extent of intertidal habitats within the estuary (33% based on habitat maps reported in Needham *et al.*⁵⁸), we calculate that unvegetated, intertidal flats account for approximately 8% of the total CO₂ emissions within estuaries, 1% of the CH₄ emissions, and 24% of the N₂O emissions (Table 6).

Habitat	Area (m ²)	% of total estuary	Mean net flux (μmol m ⁻² h ⁻¹)			Annual net flux (mol yr ⁻¹) in Tairua			Proportion of flux from each habitat		
			CO ₂	CH ₄	N ₂ O	CO ₂	CH ₄	N ₂ O	CO ₂	CH ₄	N ₂ O
Intertidal unvegetated flat	3,200,000	48%	530 ^[1,2]	0.095 ^[1,3]	0.36 ^[1,3,5,13]	1697	0.304	1.155	0.08	0.01	0.24
Subtidal unvegetated flat	1,315,000	20%	8060 ^[2]	7.2 ^[4]	0.81 ^[5]	10600	9.468	1.065	0.52	0.18	0.22
Mangroves	361,000	5%	22917 ^[6]	74 ^[7]	0.44 ^[8]	8273	26.71	0.1588	0.40	0.51	0.03
Seagrass	1,307,000	20%	-1041 ^[9]	11 ^[10]	0.71 ^[5]	-1361	14.38	0.9214	-0.07	0.27	0.19
Salt Marsh	417,000	6%	3122 ^[11]	3.5 ^[12]	3.48 ^[13,14]	1302	1.460	1.451	0.06	0.03	0.31
Total	6,600,000	100%				20510	52.32	4.752	1	1	1

Table 6. Fluxes of GHGs in Tairua Harbour. Areas are based of the mapping carried out by Needham *et al.*⁵⁸. Where possible, fluxes from New Zealand studies were used. When that data was not available, fluxes from estuaries at similar latitudes were used. Mean fluxes are the mean net flux throughout a day, and account for tidal and diurnal variation, including fluxes between emerged and submerged periods, and (where appropriate) photosynthetically active and dark conditions. 1 - This study; 2 - Thrush *et al.*, submitted; 3 - Li *et al.*, 2019; 4 - Abril & Borges, 2004; 5 - Murray, Erler & Eyre, 2015; 6 - Bulmer *et al.*, 2017; 7 - Chen *et al.*, 2010; 8 - Livesly & Andrusiak, 2012; 9 - Drylie *et al.*, 2017; 10 - Bahlmann, 2015; 11 - Lovelock *et al.*, 2017; 12 - Poffenberger *et al.*, 2001; 13 - Wang *et al.*, 2006; 14 - Tang, 2016.

Conclusions

This study has shown that nutrient enrichment increases GHG fluxes from emerged intertidal flats (increasing CO₂ uptake under light emissions, but also increasing the emission of CH₄ and N₂O). These results suggest that increased nitrogen enrichment of estuarine systems will likely lead to increased emission of GHGs, contributing to increased global GHG emissions and potentially exacerbating the impact of climate change. This study has also shown that emerged GHG fluxes from intertidal flats are an important component of estuarine GHG fluxes, particularly in estuaries where intertidal flats cover significant a significant proportion of the estuary. Finally, our study demonstrates that tidal state (submerged vs emerged) needs to be carefully considered when upscaling estimates of GHG emissions from intertidal flats, as directions and magnitudes of GHG fluxes may differ between tidal emergence and submergence.

Received: 27 June 2019; Accepted: 15 January 2020;

Published online: 21 April 2020

References

- Abril, G. & Borges, A. V. Carbon dioxide and methane emissions from estuaries, in *Greenhouse gas emissions—fluxes and processes*, Springer. p. 187–207 (2005).
- Li, X. *et al.* Salinity stress changed the biogeochemical controls on CH₄ and N₂O emissions of estuarine and intertidal sediments. *Science of The Total Environment* **652**, 593–601 (2019).
- Murray, R. H., Erler, D. V. & Eyre, B. D. Nitrous oxide fluxes in estuarine environments: response to global change. *Global change biology* **21**(9), 3219–3245 (2015).
- Vieillard, A. & Fulweiler, R. Tidal pulsing alters nitrous oxide fluxes in a temperate intertidal mudflat. *Ecology* **95**(7), 1960–1971 (2014).
- Cahoon, L. B. The role of benthic microalgae in neritic ecosystems, in *Oceanography and Marine Biology, An Annual Review, Volume 37*, CRC Press. p. 55–94 (2014).
- Heggie, K. & Savage, C. Nitrogen yields from New Zealand coastal catchments to receiving estuaries. *New Zealand Journal of Marine and Freshwater Research* **43**(5), 1039–1052 (2009).
- Thrush, S. *et al.* Muddy waters: elevating sediment input to coastal and estuarine habitats. *Frontiers in Ecology and the Environment* **2**(6), 299–306 (2004).
- Thrush, S. F. *et al.* *The many uses and values of estuarine ecosystems*. Ecosystem services in New Zealand—conditions and trends. Manaaki Whenua Press, Lincoln, New Zealand (2013).
- Billerbeck, M. *et al.* Surficial and deep pore water circulation governs spatial and temporal scales of nutrient recycling in intertidal sand flat sediment. *Marine Ecology Progress Series* **326**, 61–76 (2006).
- Wang, D. *et al.* Summer-time denitrification and nitrous oxide exchange in the intertidal zone of the Yangtze Estuary. *Estuarine, Coastal and Shelf Science* **73**(1–2), 43–53 (2007).
- Drylie, T. P. *et al.* Benthic primary production in emerged intertidal habitats provides resilience to high water column turbidity. *Journal of sea research* **142**, 101–112 (2018).
- Cammen, L. M. Annual bacterial production in relation to benthic microalgal production and sediment oxygen uptake in an intertidal sandflat and an intertidal mudflat. *Marine ecology progress series. Oldendorf* **71**(1), 13–25 (1991).
- Lara, M. *et al.* Microscale drivers of oxygen dynamics during emersion: Microphytobenthic production, sediment compaction and shifts on diffusivity. In *EGU General Assembly Conference Abstracts* (2018).
- Hohaia, A. K. *Effects of terrestrial sediment on the burial behaviour of post-settlement Macomona liliiana*. Auckland University of Technology (2012).
- Thrush, S. F. *et al.* Functional role of large organisms in intertidal communities: community effects and ecosystem function. *Ecosystems* **9**(6), 1029–1040 (2006).
- Cloern, J. E. *et al.* Human activities and climate variability drive fast-paced change across the world's estuarine-coastal ecosystems. *Global Change Biology* **22**(2), 513–529 (2016).
- Galloway, J. N. *et al.* Nitrogen cycles: past, present, and future. *Biogeochemistry* **70**(2), 153–226 (2004).
- Hume, T. M. *et al.* A controlling factor approach to estuary classification. *Ocean & coastal management* **50**(11–12), 905–929 (2007).
- Inglis, G. J. *et al.* Using habitat suitability index and particle dispersion models for early detection of marine invaders. *Ecological Applications* **16**(4), 1377–1390 (2006).

20. Morrison, M. *A review of the natural marine features and ecology of Whangarei Harbour*. National Institute of Water & Atmospheric Research (2003).
21. Millar, A. S. *Hydrology and Surficial Sediments of Whangarei Harbour: A Thesis Submitted in Partial Fulfilment of the Requirements for the Degree of Master of Science in Earth Sciences at the University of Waikato*. University of Waikato (1980).
22. Lundquist, C. & Broekhuizen, N. *Predicting suitable shellfish restoration sites in Whangarei Harbour. Larval dispersal modelling and verification. Report prepared for Ministry of Science Innovation Envirolink Fund to Northland Regional Council*. 2012. (2014).
23. Lundquist, C. J. *et al.* Changes in benthic community structure and sediment characteristics after natural recolonisation of the seagrass *Zostera muelleri*. *Scientific reports* **8**(1), 13250 (2018).
24. Larcombe, M. F. *Distribution and Recognition of Intertidal Organisms in the Whangateau Harbour, and: A Classification for Sheltered Soft Shores*. Zoology—University of Auckland (1968).
25. Council, A. R. *Ecological communities and habitats of Whangateau Harbour* (2009).
26. Hume, T. M. & Herdendorf, C. E. *Factors controlling tidal inlet characteristics on low drift coasts*. *Journal of Coastal Research*, p. 355–375 (1992).
27. Alan M. Sherwood & Campbell, S. Nelson. Surficial sediments of Raglan Harbour. *New Zealand Journal of Marine and Freshwater Research* **13**(4), 475–496 (2010).
28. Douglas, E. J. *et al.* Macrofaunal functional diversity provides resilience to nutrient enrichment in coastal sediments. *Ecosystems* **20**(7), 1324–1336 (2017).
29. Douglas, E. J. *et al.* Sedimentary environment influences ecosystem response to nutrient enrichment. *Estuaries and coasts* **41**(7), 1994–2008 (2018).
30. Hamilton, D. Greenhouse gas fluxes on emerged, unvegetated intertidal flats, in *Institute of Marine Science*. University of Auckland (2019).
31. Lohrer, A. *et al.* Ecosystem functioning in a disturbance-recovery context: contribution of macrofauna to primary production and nutrient release on intertidal sandflats. *Journal of Experimental Marine Biology and Ecology* **390**(1), 6–13 (2010).
32. Sartory, D. & Grobbelaar, J. Extraction of chlorophyll a from freshwater phytoplankton for spectrophotometric analysis. *Hydrobiologia* **114**(3), 177–187 (1984).
33. Hansson, L. A. Chlorophyll a determination of periphyton on sediments: identification of problems and recommendation of method. *Freshwater Biology* **20**(3), 347–352 (1988).
34. Joint, I. Microbial production of an estuarine mudflat. *Estuarine and Coastal Marine Science* **7**(2), 185–195 (1978).
35. Bittar, T. B. *et al.* Seasonal dynamics of dissolved, particulate and microbial components of a tidal saltmarsh-dominated estuary under contrasting levels of freshwater discharge. *Estuarine, Coastal and Shelf Science* **182**, 72–85 (2016).
36. Mook, D. H. & Hoskin, C. M. Organic determinations by ignition: caution advised. *Estuarine, Coastal and Shelf Science* **15**(6), 697–699 (1982).
37. Pratt, D. R. *et al.* The effects of short-term increases in turbidity on sandflat microphytobenthic productivity and nutrient fluxes. *Journal of sea research* **92**, 170–177 (2014).
38. Underwood, G. & Kromkamp, J. *Primary Production by Phytoplankton and Microphytobenthos in Estuaries*. *Advances in Ecological# 12 in G/WResearch*. Elsevier (1999).
39. Kang, J. *et al.* Insights into Macroinvertebrate burrowing Activity and Methane Flux in Tidal Flats. *Journal of Coastal Research* **85**(sp1), 681–685 (2018).
40. Griggs, D. J. & Noguier, M. Climate change 2001: the scientific basis. Contribution of working group I to the third assessment report of the intergovernmental panel on climate change. *Weather* **57**(8), 267–269 (2002).
41. Hargrave, B. T. Coupling carbon flow through some pelagic and benthic communities. *Journal of the Fisheries Board of Canada* **30**(9), 1317–1326 (1973).
42. Thrush, S. *et al.* Cumulative stressors reduce the self-regulating capacity of coastal ecosystems. *Ecological Applications*. **Submitted**.
43. Vermaat, J. E. & Verhagen, F. C. Seasonal variation in the intertidal seagrass *Zostera noltii* Hornem.: coupling demographic and physiological patterns. *Aquatic Botany* **52**(4), 259–281 (1996).
44. Carroll, J. L. & Wells, R. M. Strategies of anaerobiosis in New Zealand infaunal bivalves: adaptations to environmental and functional hypoxia. *New Zealand Journal of Marine and Freshwater Research* **29**(2), 137–146 (1995).
45. Kaartokallio, H. *et al.* Bacterial production, abundance and cell properties in boreal estuaries: relation to dissolved organic matter quantity and quality. *Aquatic Sciences* **78**(3), 525–540 (2016).
46. Gelesh, L. *et al.* Methane concentrations increase in bottom waters during summertime anoxia in the highly eutrophic estuary, Chesapeake Bay, USA. *Limnology and Oceanography* **61**(S1), S253–S266 (2016).
47. Howarth, R. W., Santoro, R. & Ingraffea, A. Methane and the greenhouse-gas footprint of natural gas from shale formations. *Climatic Change* **106**(4), 679 (2011).
48. Lohrer, A. M., Thrush, S. F. & Gibbs, M. M. Bioturbators enhance ecosystem function through complex biogeochemical interactions. *Nature* **431**(7012), 1092 (2004).
49. Migné, A. *et al.* Spatial and temporal variability of CO₂ fluxes at the sediment–air interface in a tidal flat of a temperate lagoon (Arcachon Bay, France). *Journal of sea research* **109**, 13–19 (2016).
50. Allen, D. E. *et al.* Spatial and temporal variation of nitrous oxide and methane flux between subtropical mangrove sediments and the atmosphere. *Soil Biology and Biochemistry* **39**(2), 622–631 (2007).
51. Bonaglia, S. *et al.* Methane fluxes from coastal sediments are enhanced by macrofauna. *Scientific reports* **7**(1), 13145 (2017).
52. Jones, H. F. E. *The ecological role of the suspension feeding bivalve, Austrovenus stutchburyi, in estuarine ecosystems*. University of Waikato (2011).
53. Bulmer, R. H., Lundquist, C. & Schwendenmann, L. Sediment properties and CO₂ efflux from intact and cleared temperate mangrove forests. *Biogeosciences* **12**(20), 6169–6180 (2015).
54. Mermillod-Blondin, F. & Rosenberg, R. Ecosystem engineering: the impact of bioturbation on biogeochemical processes in marine and freshwater benthic habitats. *Aquatic Sciences* **68**(4), 434–442 (2006).
55. Migné, A. *et al.* A closed-chamber CO₂-flux method for estimating intertidal primary production and respiration under emersed conditions. *Marine Biology* **140**(4), 865–869 (2002).
56. Chen, X. & Slater, L. Methane emission through ebullition from an estuarine mudflat: 1. A conceptual model to explain tidal forcing based on effective stress changes. *Water Resources Research* **52**(6), 4469–4485 (2016).
57. Murray, N. J. *et al.* The global distribution and trajectory of tidal flats. *Nature* **565**(7738), 222 (2019).
58. Needham, H. R. *et al.* *Intertidal habitat mapping for ecosystem goods and services: Tairua harbour* (2014).
59. Garcias-Bonet, N. & Duarte, C. M. Methane production by seagrass ecosystems in the Red Sea. *Frontiers in Marine Science* **4**, 340 (2017).
60. Bahlmann, E. *et al.* Tidal controls on trace gas dynamics in a seagrass meadow of the Ria Formosa lagoon (southern Portugal). *Biogeosciences* **12**(6), 1683–1696 (2015).
61. Bulmer, R. H. *et al.* Sediment carbon and nutrient fluxes from cleared and intact temperate mangrove ecosystems and adjacent sandflats. *Science of the Total Environment* **599**, 1874–1884 (2017).
62. Chen, G., Tam, N. & Ye, Y. Summer fluxes of atmospheric greenhouse gases N₂O, CH₄ and CO₂ from mangrove soil in South China. *Science of the Total Environment* **408**(13), 2761–2767 (2010).

63. Poffenbarger, H. J., Needelman, B. A. & Megonigal, J. P. Salinity influence on methane emissions from tidal marshes. *Wetlands* **31**(5), 831–842 (2011).
64. Lovelock, C. E., Fourqurean, J. W. & Morris, J. T. Modeled CO₂ emissions from coastal wetland transitions to other land uses: tidal marshes, mangrove forests, and seagrass beds. *Frontiers in Marine Science* **4**, 143 (2017).
65. Yang, W. H. & Silver, W. L. Gross nitrous oxide production drives net nitrous oxide fluxes across a salt marsh landscape. *Global change biology* **22**(6), 2228–2237 (2016).

Acknowledgements

This research was completed as part of the requirements for a MSc degree to D.J.H. at the University of Auckland. Additional funding for this study was provided by the NIWA Strategic Science Investment Fund, project #COME1903. We acknowledge the contributions of researchers from the University of Auckland, the University of Waikato and NIWA who contributed to the experimental design and site set up for nutrient treatments within a national experiment on multiple stressors, funded by the Ministry of Business, Employment and Innovation under the New Zealand National Science Challenge ‘Sustainable Seas’ (MBIE Contract #CO1X1515, Tipping Points project).

Author contributions

Gas and sediment samples were collected by D.J.H., R.H.B. and C.J.L. Analysis of gas samples was carried out by D.J.H. and L.S. Sediment samples were analysed by D.J.H. and L.S. D.J.H. led data analysis and the writing of the manuscript. All authors contributed to the discussion and interpretation of the data collected, and to the writing of the manuscript.

Competing interests

The authors declare no competing interests.

Additional information

Supplementary information is available for this paper at <https://doi.org/10.1038/s41598-020-62215-4>.

Correspondence and requests for materials should be addressed to C.J.L.

Reprints and permissions information is available at www.nature.com/reprints.

Publisher’s note Springer Nature remains neutral with regard to jurisdictional claims in published maps and institutional affiliations.



Open Access This article is licensed under a Creative Commons Attribution 4.0 International License, which permits use, sharing, adaptation, distribution and reproduction in any medium or format, as long as you give appropriate credit to the original author(s) and the source, provide a link to the Creative Commons license, and indicate if changes were made. The images or other third party material in this article are included in the article’s Creative Commons license, unless indicated otherwise in a credit line to the material. If material is not included in the article’s Creative Commons license and your intended use is not permitted by statutory regulation or exceeds the permitted use, you will need to obtain permission directly from the copyright holder. To view a copy of this license, visit <http://creativecommons.org/licenses/by/4.0/>.

© The Author(s) 2020